

# UCLA

## UCLA Previously Published Works

### Title

Prediction of Intracranial Atherosclerotic Disease-Related Large-Vessel Occlusion Stroke on the Basis of Novel Cerebral Blood Volume Parameters.

### Permalink

<https://escholarship.org/uc/item/71n8q9gq>

### Journal

Journal of the American Heart Association: Cardiovascular and Cerebrovascular Disease, 13(2)

### Authors

Koh, Seungyon

Park, So

Liebeskind, David

et al.

### Publication Date

2024-01-16











### DOI

10.1161/JAHA.123.030936

Peer reviewed

ORIGINAL RESEARCH

# Prediction of Intracranial Atherosclerotic Disease-Related Large-Vessel Occlusion Stroke on the Basis of Novel Cerebral Blood Volume Parameters

Seungyon Koh , MD; So Young Park , MD; David S. Liebeskind , MD; Jin Wook Choi , MD, PhD; Han Ki Kim , MD; Jun Young Choi , MD, PhD; Min Kim , MD; Seong-Joon Lee , MD, PhD; Ji Man Hong , MD, PhD; Jin Soo Lee , MD, PhD

**BACKGROUND:** Mechanical thrombectomy is an effective treatment method for large-vessel occlusion stroke (LVOS); however, it has limited efficacy for intracranial atherosclerotic disease (ICAD)-related LVOS. We investigated the use of cerebral blood volume (CBV) maps for identifying ICAD as the underlying cause of LVOS before the initiation of endovascular treatment (EVT).

**METHODS AND RESULTS:** We reviewed clinical and imaging data from patients who presented with LVOS and underwent endovascular treatment between January 2011 and May 2021. The CBV patterns were analyzed to identify an increase in CBV within the hypoperfused area and estimate infarct patterns within the area of decreased CBV. Comparisons were made between the patients with an increase in CBV and those without, and among the estimated infarct patterns: territorial, cortical wedge, basal ganglia-only, subcortical, and normal CBV. Overall, 243 patients were included. CBV increase in the hypoperfused area was observed in 23.5% of patients. A significantly higher proportion of ICAD was observed in those with increased CBV than in those without (56.4% versus 19.8%;  $P < 0.001$ ). Regarding the estimated infarct patterns on the CBV, ICAD was most frequently observed in the normal CBV group (territorial, 14.9%; cortical wedge, 10.0%; basal ganglia-only, 43.8%; subcortical, 35.7%; normal, 61.7%). CBV parameters, including “an increase in CBV,” “normal CBV infarct pattern,” and “an increase in CBV or normal CBV infarct pattern composite,” were independently associated with ICAD.

**CONCLUSIONS:** An increased CBV or normal CBV pattern may be associated with ICAD LVOS on the pretreatment perfusion imaging.

**Key Words:** cerebral blood volume ■ emergent large-vessel occlusion ■ intracranial atherosclerotic disease ■ magnetic resonance imaging ■ perfusion map

Endovascular treatment (EVT) has been proven to be an effective method for treating large-vessel occlusion stroke (LVOS) in several randomized controlled trials and is now considered the gold standard.<sup>1,2</sup> Mechanical thrombectomy, a primary EVT technique, is mainly effective in treating cerebral emboli principally caused by cardioembolism. However,

intracranial atherosclerotic disease (ICAD)-related LVOS, which is more prevalent in Asian populations, is often associated with the limited effectiveness of mechanical thrombectomy due to residual stenosis after thrombus removal.<sup>3,4</sup>

Identifying the underlying ICAD as a cause of LVOS before treatment is believed to be important for various

Correspondence to: Jin Soo Lee, MD, PhD, Department of Neurology, Ajou University School of Medicine, Ajou University Hospital Gyunggi-do, Suwon, Youngtong-gu, Worldup-ro, 16499, Republic of Korea. Email: [jinsoo22@gmail.com](mailto:jinsoo22@gmail.com)

This manuscript was sent to Neel S. Singhal, MD, PhD, Associate Editor, for review by expert referees, editorial decision, and final disposition.

Supplemental Material is available at <https://www.ahajournals.org/doi/suppl/10.1161/JAHA.123.030936>

For Sources of Funding and Disclosures, see page 10.

© 2023 The Authors. Published on behalf of the American Heart Association, Inc., by Wiley. This is an open access article under the terms of the [Creative Commons Attribution-NonCommercial-NoDerivs](https://creativecommons.org/licenses/by-nc-nd/4.0/) License, which permits use and distribution in any medium, provided the original work is properly cited, the use is non-commercial and no modifications or adaptations are made.

JAHA is available at: [www.ahajournals.org/journal/jaha](http://www.ahajournals.org/journal/jaha)

## CLINICAL PERSPECTIVE

### What Is New?

- A significantly higher proportion of intracranial atherosclerotic disease was observed in those with increased cerebral blood volume (CBV) on an ipsilesional hypoperfused area of large-vessel occlusion.
- CBV parameters, including “an increase in CBV,” “normal CBV infarct pattern,” and “an increase in CBV or normal CBV infarct pattern composite,” were independently associated with intracranial atherosclerotic disease.

### What Are the Clinical Implications?

- CBV maps can be a useful point-of-care neuroimaging tool for predicting intracranial atherosclerotic disease as an underlying cause of large-vessel occlusion stroke.
- New randomized controlled trials for intracranial atherosclerotic disease large-vessel occlusion stroke may proceed on the basis of a combination of current CBV parameters and other strong predictors.

## Nonstandard Abbreviations and Acronyms

<b>CBV</b>	cerebral blood volume
<b>EVT</b>	endovascular treatment
<b>ICAD</b>	intracranial atherosclerotic disease
<b>LVOS</b>	large-vessel occlusion stroke
<b>MRP</b>	magnetic resonance perfusion
<b>mRS</b>	modified Rankin Scale
<b>MTT</b>	mean transit time
<b>NIHSS</b>	National Institute of Health Stroke Scale
<b>T<sub>max</sub></b>	time-to-max

reasons. First, it would be helpful in device and technique selection.<sup>5</sup> This proactive approach enables customization of procedural strategies by accounting for potential challenges posed by ICAD, such as the risk of residual stenosis, or the necessity of supplementary therapies, such as tirofiban infusion, to enhance outcomes. Moreover, the preprocedural identification of ICAD LVOS is important, considering the absence of randomized controlled trials exclusively examining the efficacy of a novel interventional technique or device in ICAD LVOS. In this context, given the inherent challenges posed by residual thrombosis and the heightened risk of reocclusion, meticulous patient selection becomes paramount. A pivotal initial step involves

formulating a rigorous diagnostic framework for ICAD to accurately differentiate it from its mimics and enrolling patients with genuine ICAD pathology, thus ensuring the authenticity and relevance of the subsequent randomized controlled trial findings.

Cerebral blood volume (CBV) parameter maps on perfusion imaging reflect the blood reservoir mediated by vasodilatation and are associated with the recruitment of collaterals following acute intracranial arterial occlusion.<sup>6</sup> Furthermore, a significant decrease in CBV has been considered an alternative method for determining the infarct core.<sup>7</sup> It is assumed that ICAD LVOS is associated with increased vascular reservoirs and collaterals, as well as a lower initial infarct burden, as determined by baseline CBV maps, compared with embolic LVOS.

The current study explored the clinical and imaging point-of-care factors observed in LVOS, with particular attention to the CBV state on baseline perfusion maps. Specifically, we used magnetic resonance perfusion (MRP) maps of the CBV as an imaging biomarker to predict underlying ICAD as a cause of LVOS.

## METHODS

### Study Design and Patients

Clinical and imaging data from patients who presented with LVOS and underwent EVT from January 2011 to May 2021 were retrospectively reviewed from a consecutively enrolled registry at Ajou University Hospital (Suwon, Republic of Korea). The current study was reviewed and approved by the institutional review board of Ajou University Medical Center (AJIRB-MED-MDB-21-201), with a waiver for informed consent due to the retrospective nature of the study. The data that support the findings of this study are available from the corresponding author upon reasonable request.

Patients with anterior circulation unilateral LVOS were selected, whereas those with posterior circulation stroke and bilateral anterior LVOS were excluded. Patients with pre-EVT MRP images were included, excluding those without pre-EVT MRP, with limited MRP image quality due to inappropriate contrast injection, and without calculated MRP CBV maps.

Variables such as baseline demographics, medical history, vital signs at presentation, laboratory test results at presentation, initial National Institute of Health Stroke Scale (NIHSS) score, imaging findings including Alberta Stroke Program Early Computed Tomography Score and occlusion site, and presumed occlusion causes were collected from the registry. Truncal-type occlusion on baseline computed tomography (CT) was evaluated according to previous reports. A truncal-type occlusion refers to sparing of the bifurcation

site of thrombotic occlusion, potentially indicating an ICAD-related occlusion, as opposed to an embolic occlusion.<sup>8,9</sup> The final causes were classified as ICAD-related or non-ICAD-related. The definition of ICAD in this study was a fixed focal stenosis documented during EVT and confirmed on short-term follow-up CT angiography.<sup>10,11</sup>

## Magnetic Resonance Imaging Acquisition and Image Analysis

Magnetic resonance imaging was performed with a 3T magnetic resonance scanner (Intera Achieva; Philips Healthcare, Best, The Netherlands) using a 16-channel neurovascular head coil. Perfusion-weighted imaging was performed using dynamic susceptibility-weighted contrast-enhanced MRP imaging. A contrast agent was administered using a standard dose of 0.1 mmol/kg gadopentetate dimeglumine at a rate of 4 mL/s with an MR imaging-compatible power injector (Spectris; Medrad, Pittsburgh, PA), followed by a 20-mL bolus of saline at the same injection rate. Multiple parameter maps were created for each participant using a software package (NordicICE; NordicNeuroLab, Bergen, Norway). Perfusion processing was performed using selection of the arterial input function and a convolution/deconvolution method in a delay-dependent manner. Images were analyzed using a commercial image-viewing software (Picture Archiving and Communication System; Maroview 5.3 Infinite Co., Seoul, Republic of Korea). Two independent neurologists (S.K. and S.Y.P.) who were blinded to the clinical information inspected the images and evaluated CBV variables.

## Definitions of CBV Parameters

Figure 1 illustrates the CBV patterns used in this study. The MRP CBV variables were evaluated in 2 distinct and exclusive categories: (1) cases with an increase in CBV versus those with no increase in CBV; and (2) infarct patterns estimated on the basis of areas of decreased CBV and normal CBV patterns.

First, the hypoperfused area was visually identified by examining the mean transit time (MTT) map, allowing for lateralization to determine whether the region was situated on the right or left side. Subsequently, an increase in CBV was depicted on the ipsilesional hemisphere with the delayed perfusion on the MTT map. An increased area on the CBV map, relative to a corresponding region in the contralesional hemisphere, was deemed indicative of an increase in CBV regardless of whether there was a reduced CBV in the center. Conversely, similar, comparable, or equivocal CBV levels without a notable increase in CBV compared with the corresponding region in the contralesional hemisphere were categorized as nonincrease in CBV.

Second, estimated infarct patterns on MRP CBV were visually evaluated by inspecting CBV color scale levels to include the area with a clear and significant decrease in CBV. The infarct patterns were identified upon a clear reduction in CBV within the hypoperfused area of the MTT map. Discernible bluish to purple-colored margins were defined as infarcted areas. Infarct patterns were classified into 5 groups: territorial, cortical wedge, basal ganglia-only, subcortical, and normal CBV patterns. The territorial pattern signified a decrease in CBV within the occluded vascular territory, covering both cortical and subcortical zones. The cortical wedge pattern was characterized by a wedge-shaped region of decreased CBV, which was considered a specific segment of the vascular territory and predominantly influences the cortex rather than the subcortex. In the basal ganglia-only pattern, the reduction in CBV was limited solely to the basal ganglia region. The subcortical pattern displayed decreased CBV primarily within the subcortical region of the hypoperfused area. Finally, the normal infarct pattern was recognized by the absence of definitive CBV reduction within the hypoperfused area.

## Statistical Analysis

Comparative analyses were performed (1) between the groups with increased or nonincreased CBV and (2) among the estimated infarct patterns on CBV. The data are presented as mean  $\pm$  SD, frequency (percentage), or median [interquartile range]. Statistical significance was set at  $P < 0.05$ . Continuous variables were compared using either the Student *t*-test or the Mann-Whitney *U* test according to the parametricity of the data, while categorical variables were subjected to the chi-square test or Fisher's exact test. The normality of continuous variable distributions was evaluated using the Shapiro-Wilk test. According to the comparative analysis results, an increase in CBV, a normal CBV pattern, and a composite of both parameters were incorporated into the multivariable regression analyses for ICAD prediction. For the multivariable logistic regression analyses, covariables were chosen on the basis of comparative analysis and expert opinions, including age, absence of atrial fibrillation, NIHSS, hemoglobin levels, and truncal-type occlusion. Interrater agreement of the rated CBV variables was calculated as kappa values (95% CIs).

## RESULTS

### Population

The inclusion and exclusion criteria of patients are presented in Figure 2. Overall, 545 patients diagnosed with LVOS who underwent EVT between January



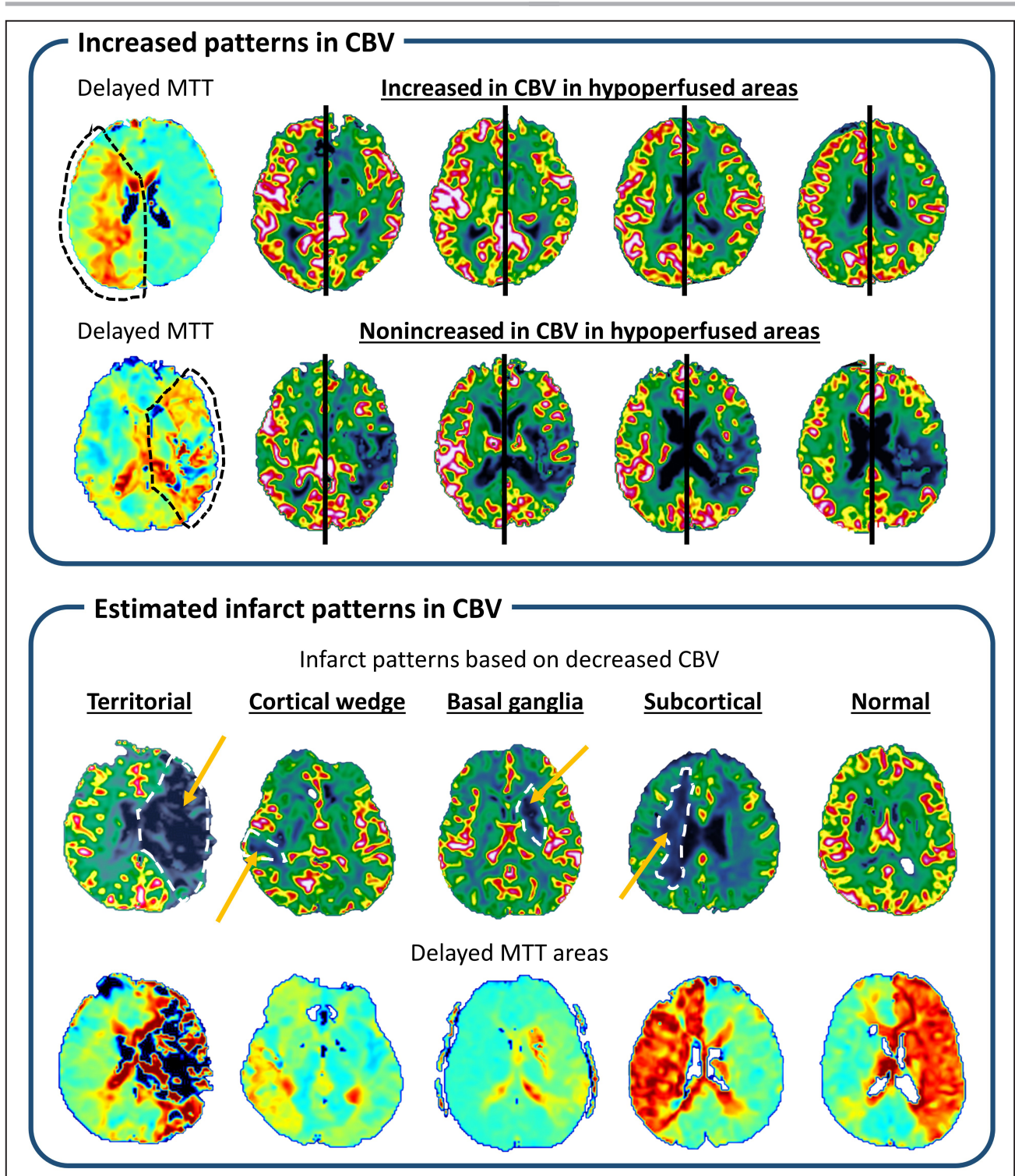


**Figure 1. Grading of CBV increase in hyperperfused areas.**

The hyperperfused area was identified through the MTT map. The area of a clear and significant increase in MTT within the presumably occluded MCA territory was considered the hyperperfused area. A focal increase is identified by comparing the contralateral hemisphere’s analogous area and visually inspected with the color scale in CBV. Decreased CBV is commonly seen in most patients with stroke, as justified by nature; therefore, it was graded as not increased. Further, comparable, similar, or equivocal CBV without any distinguished and outstanding increase in CBV compared with the corresponding contralateral hemisphere was defined as not increased. CBV indicates cerebral blood volume; and MTT, mean transit time.

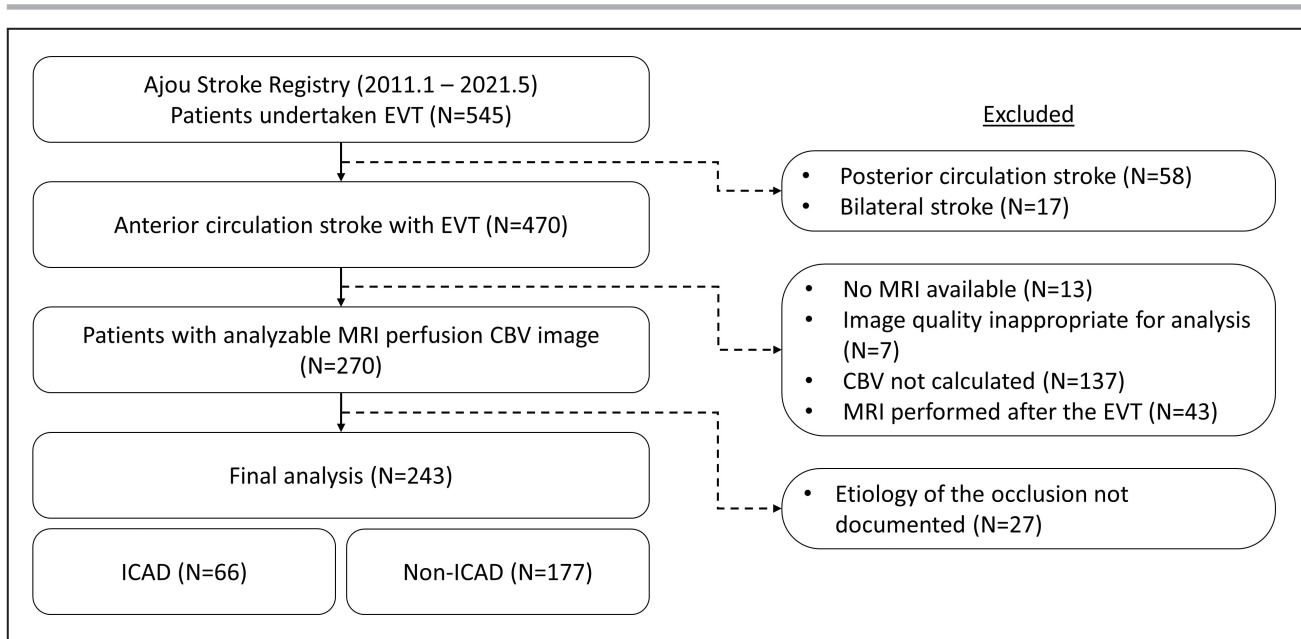


**Figure 2. Study flowchart.**

EVT indicates endovascular treatment; MRI, magnetic resonance imaging; CBV, cerebral blood volume; and ICAD, intracranial atherosclerotic disease.

2011 and May 2021 were included in the registry. After applying the exclusion criteria, the final data set comprised 243 patients. The mean age of the patients was  $66.73 \pm 13.67$  years, and 135 (55.56%) were men.

### Increase in CBV

An increase in CBV in the hypoperfused area was observed in 57 (23.5%) patients. The interrater agreement of the increased CBV by 2 independent raters was 0.4191 (95% CI, 0.2933–0.5448). Comparative analyses were performed between groups with presence and absence of increased CBV (Table 1). Diabetes (20.0% versus 35.1%;  $P=0.0301$ ) and smoking (15.3% versus 36.8%;  $P<0.001$ ) were more frequently observed in the increased CBV subset, whereas atrial fibrillation was less frequently observed (52.7% versus 29.8%;  $P=0.0041$ ). The initial NIHSS score was lower (16.5 [13–19] versus 11.5 [7.75–15.25];  $P<0.001$ ), the initial Alberta Stroke Program Early Computed Tomography Score was higher (8 [6–9] versus 9 [7–10];  $P=0.0024$ ), and truncal-type occlusions were more frequently observed (14.9% versus 41.8%;  $P<0.001$ ). Regarding the underlying cause, a significantly higher proportion of ICAD was observed in the group with an increase in CBV (19.8% versus 56.4%;  $P<0.001$ ). The median 3-month modified Rankin Scale (mRS) score was more favorable in the increased CBV group (3 [1–5] versus 1.5 [0–4];  $P=0.0092$ ). In addition, after ICAD and baseline variables were adjusted, increased CBV showed an independent association with good clinical outcome (3-month mRS, 0–2) (Tables S1 and S2).

### Estimated Infarct Patterns on CBV

As for the estimated infarct patterns based on the severely decreased CBV area, 127 (52.3%) were identified as territorial, 22 (9.1%) as cortical wedge, 16 (6.6%) as basal ganglia-only, 30 (12.4%) as subcortical infarct patterns, and 48 (19.8%) as normal patterns. A comparative analysis was conducted between the groups (Table 2). Statistical significance was found for atrial fibrillation, smoking, initial NIHSS, Alberta Stroke Program Early Computed Tomography Score, truncal-type occlusion, ICAD as an underlying cause, and 3-month mRS score. Notably, the normal CBV pattern showed a significantly lower rate of atrial fibrillation (territorial, 49.2%; cortical wedge, 72.7%; basal ganglia-only, 50.0%; subcortical, 50.0%; normal, 27.7%;  $P=0.0099$ ). The initial NIHSS score was lower in the basal ganglia-only and normal CBV groups ( $16.9 \pm 3.87$  versus  $14.77 \pm 5.01$  versus  $12.19 \pm 5.37$  versus  $15.33 \pm 4.38$  versus  $11.28 \pm 5.77$ ;  $P<0.001$ ). The Alberta Stroke Program Early Computed Tomography Score was significantly lower in the territorial group (7 [5–8.25] versus 9 [8, 9] versus 8 [7–9] versus 9 [7–9] versus 9 [8–10],  $P<0.001$ ). Truncal-type occlusions were observed more frequently in the normal CBV group (9.32% versus 5.0% versus 37.5% versus 28.6% versus 48.9%,  $P<0.001$ ). Among CBV-based infarct patterns, cortical wedge, subcortical, and normal patterns accounted for a high proportion of scattered infarct pattern based on diffusion-weighted imaging, whereas CBV-based territorial infarct pattern was mostly associated with territorial infarct pattern on diffusion-weighted imaging. ICAD as an underlying

**Table 1. Comparative Analysis Between Patients With an Increase and Nonincrease in CBV**

	Nonincrease (N=186)	Increase (N=57)	P value
Age, y	68.5 (60–79)	62 (53–76)	0.0351
Sex, male	99 (53.23)	36 (63.16)	0.2428
Hypertension	115 (62.16)	30 (52.63)	0.2588
Diabetes	37 (20)	20 (35.09)	0.0301
Atrial fibrillation	97 (52.72)	17 (29.82)	0.0041
Dyslipidemia	15 (8.11)	8 (14.04)	0.282
Smoking	28 (15.3)	21 (36.84)	<0.001
Prior stroke/TIA	28 (15.05)	6 (10.53)	0.5197
Prior antiplatelet use	52 (30.23)	15 (26.79)	0.7467
Prior anticoagulation use	19 (11.05)	4 (7.14)	0.5572
Initial NIHSS	16.5 (13–19)	11.5 (7.75–15.25)	<0.001
Systolic BP, mmHg	140 (125–156)	143 (118.5–160.75)	0.6725
WBCs, $\times 10^9/L$	7.9 (6.3–10.07)	8.2 (6.6–11)	0.4666
Hemoglobin, g/dL	13.65 (12.6–14.9)	14.3 (12.5–15.2)	0.2361
Platelets, $\times 10^3/\mu L$	206 (170–246.75)	218 (178–237)	0.5536
Total cholesterol, mg/dL	158.3 $\pm$ 41.67	165.42 $\pm$ 40.72	0.2532
INR	1.05 (0.98–1.1)	1.03 (0.99–1.09)	0.4884
Glucose, mg/dL	125 (109–150)	121 (107–170)	0.6347
ASPECTS	8 (6–9)	9 (7–10)	0.0024
Occlusion site by CTA			
Overall intracranial ICA	63 (35.39)	12 (21.82)	0.2598
M1	90 (50.56)	35 (63.64)	
M2/M3	15 (8.43)	5 (9.09)	
Tandem	6 (3.37)	1 (1.82)	
Multiple	2 (1.12)	2 (3.64)	
Others	2 (1.12)	0 (0)	
Truncal-type occlusion	26 (14.94)	23 (41.82)	<0.001
Final cause			
Embolism	139 (78.53)	24 (43.64)	<0.001
ICAD	35 (19.77)	31 (56.36)	
Intractable	1 (0.56)	0 (0)	
ECAD	2 (1.13)	0 (0)	
3-mo mRS	3 (1–5)	1.5 (0–4)	0.0092

Data are presented as n (%) or median (interquartile range). ASPECTS indicates Alberta Stroke Program Early Computed Tomography Score; BP, blood pressure; CBV, cerebral blood volume; CTA, computed tomography angiography; ECAD, extracranial atherosclerotic disease; ICA, internal carotid artery; ICAD, intracranial atherosclerotic disease; INR, international normalized ratio; mRS, modified Rankin Scale; NIHSS, National Institute of Health Stroke Scale; TIA, transient ischemic attack; and WBC, white blood cell.

cause was most frequently observed in the normal CBV group (14.9% versus 10.0% versus 43.8% versus 35.7% versus 61.7%). The 3-month mRS also significantly differed among groups, with the most favorable mRS scores in the normal CBV group (4 [2–5] versus 1 [0.75–3] versus 3 [1–4] versus 2 [1–4] versus 1 [0–4];

$P=0.0033$ ). The normal CBV group showed a statistical tendency toward good clinical outcomes; however, it did not reach statistical significance for proving an independent association with good clinical outcomes after adjustment (Tables S1 and S2). The interrater agreement of the normal CBV by 2 independent raters was 0.4117 (95% CI, 0.3019–0.5215).

### CBV Pattern as an ICAD Predictor

A comparison between ICAD and non-ICAD LVOS is presented in Table 3. Results from logistic regression analyses show that each CBV parameter, including “an increase in CBV,” “normal CBV infarct pattern,” and “an increase of CBV or normal CBV infarct pattern composite,” had an independent association with ICAD (Table 4). The regression model incorporating the increase in CBV (odds ratio, 2.81 [95% CI, 1.27–6.45]) showed an area under the receiver operating characteristic curve of 0.832, the normal CBV pattern (odds ratio, 2.85 [95% CI, 1.20–6.75]) showed an area under the receiver operating characteristic curve of 0.828, and the CBV composite parameter (odds ratio, 3.13 [95% CI, 1.43–6.84]) showed an area under the receiver operating characteristic curve of 0.834.

## DISCUSSION

The current study explored novel factors that predict ICAD as an underlying cause in patients with LVOS, with a particular focus on CBV states in the pre-EVT perfusion map. The central premise of this study is that the increase in CBV reflects the presence of increased vascular reservoirs and collaterals, whereas severely decreased CBV reflects the infarct core. This study used MRP CBV as an imaging biomarker to predict underlying ICAD, hypothesizing that patients with ICAD have developed vascular reservoirs by stenosis progression and that the infarct core of patients with ICAD LVOS could be smaller in cases of more sufficient collateral supply. Our results revealed that an increase of CBV in the hypoperfused area, regardless of the infarct core in the center, a normal CBV pattern among several estimated infarct patterns, and a composite of both parameters were independently associated with underlying ICAD in patients with LVOS.

Various studies have been conducted to predict ICAD as an underlying cause across different dimensions. Studies employing perfusion imaging are relatively uncommon, with a particular emphasis on time maps, such as  $T_{max}$  (time-to-max), within diverse perfusion methodologies. A prior study highlighted an autonomous association between a profile of  $T_{max} > 4$  s/ $T_{max} > 6$  s ratio  $\geq 2$  in automated CT perfusion and underlying ICAD LVOS.<sup>12</sup> In a separate study, high relative

**Table 2. Comparative Analysis Among Estimated Infarct Patterns on CBV**

	Territorial	Cortical wedge	Basal ganglia	Subcortical	Normal	P value
No. (%)	127 (52.26)	22 (9.05)	16 (6.58)	30 (12.35)	48 (19.75)	
Age, y	67 (59–78)	71.5 (60.75–78.25)	61.5 (57.5–75)	72.5 (63.25–80.75)	66 (53.75–75.25)	0.2724
Sex, male	69 (54.33)	12 (54.55)	10 (62.5)	15 (50)	29 (60.42)	0.8726
Hypertension	73 (57.94)	17 (77.27)	11 (68.75)	19 (63.33)	25 (52.08)	0.3023
Diabetes	27 (21.43)	5 (22.73)	2 (12.5)	5 (16.67)	18 (37.5)	0.1506
Atrial fibrillation	62 (49.21)	16 (72.73)	8 (50)	15 (50)	13 (27.66)	<b>0.0099*</b>
Dyslipidemia	10 (7.94)	1 (4.55)	2 (12.5)	4 (13.33)	6 (12.5)	0.6471
Smoking	17 (13.6)	3 (14.29)	3 (18.75)	8 (26.67)	18 (37.5)	<b>0.0109*</b>
Prior stroke/TIA	23 (18.11)	1 (4.55)	0 (0)	2 (6.67)	8 (16.67)	0.1206
Prior antiplatelet use	28 (23.73)	12 (57.14)	4 (25)	9 (31.03)	14 (31.82)	0.0512
Prior anticoagulation use	15 (12.71)	2 (9.52)	0 (0)	3 (10.34)	3 (6.82)	0.6203
Initial NIHSS	16.9±3.87	14.77±5.01	12.19±5.37	15.33±4.38	11.28±5.77	<b>&lt;0.001*</b>
Systolic BP, mmHg	140 (121–152)	140.5 (135.25–155.5)	148 (135–169.5)	140 (117–160)	148 (130–160)	0.2977
WBCs, ×10 <sup>9</sup> /L	8.1 (6.6–10.6)	6.8 (5.93–8.25)	8.6 (7.72–9.98)	7.25 (6.23–8.73)	8.2 (6.57–11.18)	0.1173
Hemoglobin, g/dL	13.7 (12.45–14.9)	13.55 (12.72–14.7)	14 (13.25–15.2)	13.5 (12.6–14.95)	14 (12.38–15.2)	0.7589
Platelets, ×10 <sup>3</sup> /μL	206 (172.5–248.5)	204 (163–254.25)	208 (180.75–221.25)	210.5 (173.5–239.75)	218 (176.5–239.25)	0.9345
Total cholesterol, mg/dL	157.38±41	154.95±36.61	180.44±33	163.03±40.12	160.38±47.24	0.1529
INR	1.05 (0.98–1.11)	1.02 (0.99–1.08)	1.02 (0.97–1.09)	1.04 (1.01–1.12)	1.03 (0.98–1.09)	0.6558
Glucose, mg/dL	123 (108–148.75)	129 (108.5–153.75)	120.5 (105.5–130.5)	119.5 (104.75–140)	139.5 (109.75–193)	0.0616
ASPECTS	7 (5–8.25)	9 (8–9)	8 (7–9)	9 (7–9)	9 (8–10)	<b>&lt;0.001*</b>
Occlusion site by CTA						
Overall intracranial ICA	47 (38.84)	2 (10)	5 (31.25)	12 (41.38)	9 (19.15)	NA
M1	58 (47.93)	11 (55)	10 (62.5)	13 (44.83)	33 (70.21)	
M2/M3	5 (4.13)	5 (25)	1 (6.25)	4 (13.79)	5 (10.64)	
Tandem	6 (4.96)	1 (5)	0 (0)	0 (0)	0 (0)	
Multiple	3 (2.48)	1 (5)	0 (0)	0 (0)	0 (0)	
Others	2 (1.65)	0 (0)	0 (0)	0 (0)	0 (0)	
Truncal-type occlusion	11 (9.32)	1 (5)	6 (37.5)	8 (28.57)	23 (48.94)	<b>&lt;0.001*</b>
DWI infarct pattern						
Basal ganglia only	8 (6.3)	2 (9.09)	8 (50)	8 (26.67)	6 (12.5)	NA
Border zone only	1 (0.79)	1 (4.55)	3 (18.75)	5 (16.67)	9 (18.75)	
Scattered	10 (7.87)	14 (63.64)	2 (12.5)	12 (40)	27 (56.25)	
Subcortical	0 (0)	0 (0)	0 (0)	1 (3.33)	1 (2.08)	
Territorial	107 (84.25)	3 (13.64)	2 (12.5)	2 (6.67)	2 (4.17)	
No lesion	1 (0.79)	2 (9.09)	1 (6.25)	2 (6.67)	3 (6.25)	
Final cause						
Embolism	101 (83.47)	17 (85)	9 (56.25)	18 (64.29)	18 (38.3)	NA
ICAD	18 (14.88)	2 (10)	7 (43.75)	10 (35.71)	29 (61.7)	
Intractable	1 (0.83)	0 (0)	0 (0)	0 (0)	0 (0)	
ECAD	1 (0.83)	1 (5)	0 (0)	0 (0)	0 (0)	
3-mo mRS	4 (2–5)	1 (0.75–3)	3 (1–4)	2 (1–4)	1 (0–4)	<b>0.0033*</b>

Data are presented as n (%) or median (interquartile range). ASPECTS indicates Alberta Stroke Program Early Computed Tomography Score; BP, blood pressure; CBV, cerebral blood volume; CTA, computed tomography angiography; DWI, diffusion-weighted imaging; ECAD, extracranial atherosclerotic disease; ICA, internal carotid artery; ICAD, intracranial atherosclerotic disease; INR, international normalized ratio; mRS, modified Rankin Scale; NA, not applicable; NIHSS, National Institute of Health Stroke Scale; TIA, transient ischemic attack; and WBC, white blood cell.

\*The values are statistically significant.

CBV observed on CT perfusion maps, along with a low hypoperfusion index ratio, correlated with favorable collaterals, while a lower relative CBV predicted

increased infarct growth.<sup>6</sup> In these prior studies, parameters were automatically calculated and were reported numerically. In contrast, our current study



**Table 3. Comparative Analysis Between ICAD LVOS and Other LVOS Groups**

	Non-ICAD	ICAD	P value
No. (%)	177 (72.8)	66 (27.2)	
Age, y	68 (59–79)	66 (55.25–76)	0.2466
Sex, male	92 (51.98)	43 (65.15)	0.0904
Hypertension	106 (60.23)	39 (59.09)	0.9893
Diabetes	37 (21.02)	20 (30.3)	0.1786
Atrial fibrillation	100 (56.82)	14 (21.54)	<b>&lt;0.001*</b>
Dyslipidemia	16 (9.09)	7 (10.61)	0.9109
Smoking	30 (17.24)	19 (28.79)	0.0715
Prior stroke/TIA	27 (15.25)	7 (10.61)	0.4708
Prior antiplatelet use	55 (32.54)	12 (20.34)	0.1083
Prior anticoagulation use	21 (12.43)	2 (3.39)	0.0831
Initial NIHSS	16 (13–19)	13 (9–17)	<b>&lt;0.001*</b>
Systolic BP, mmHg	140 (120–151)	148.5 (130–160.75)	<b>0.0406*</b>
WBCs, ×10 <sup>9</sup> /L	7.7 (6.2–9.7)	8.35 (7.12–10.2)	0.0911
Hemoglobin, g/dL	13.5 (12.4–14.7)	14.45 (13.03–15.28)	<b>0.0087*</b>
Platelet, ×10 <sup>3</sup> /μL	206 (169–247)	213.5 (180.5–238.5)	0.6443
Total cholesterol, mg/dL	157.16 ± 40.82	167.48 ± 42.58	0.092
INR	1.05 (0.99–1.12)	1.01 (0.98–1.07)	<b>0.0079*</b>
Glucose, mg/dL	124 (108–149.25)	124.5 (107–169.5)	0.5997
ASPECTS	8 (6–9)	8 (7–9)	0.1805
Occlusion site by CTA			
Overall intracranial ICA	53 (31.74)	22 (33.33)	0.0764
M1	83 (49.7)	42 (63.64)	
M2/M3	18 (10.78)	2 (3.03)	
Tandem	7 (4.19)	0 (0)	
Multiple	4 (2.4)	0 (0)	
Others	2 (1.2)	0 (0)	
Truncal-type occlusion	16 (9.82)	33 (50)	<b>&lt;0.001*</b>
Increase on CBV	26 (14.69)	31 (46.97)	<b>&lt;0.001*</b>
Estimated infarct pattern on CBV			
Territorial	109 (61.58)	18 (27.27)	<b>&lt;0.001*</b>
Cortical wedge	20 (11.3)	2 (3.03)	
Basal ganglia only	9 (5.08)	7 (10.61)	
Subcortical	20 (11.3)	10 (15.15)	
Normal	19 (10.73)	29 (43.94)	
DWI infarct pattern			
Basal ganglia-only	24 (13.56)	8 (12.12)	<b>&lt;0.001*</b>
Border zone only	11 (6.21)	8 (12.12)	
Scattered	36 (20.34)	29 (43.94)	
Subcortical	1 (0.56)	1 (1.52)	
Territorial	98 (55.37)	18 (27.27)	
No lesion	7 (3.95)	2 (3.03)	

(Continued)

**Table 3. Continued**

	Non-ICAD	ICAD	P value
3-mo mRS	3 (1–4)	3 (1–4.25)	0.9839

Data are presented as n (%) or median (interquartile range). ASPECTS indicates Alberta Stroke Program Early Computed Tomography Score; BP, blood pressure; CTA, computed tomography angiography; DWI, diffusion-weighted imaging; ICA, internal carotid artery; ICAD, intracranial atherosclerotic disease; INR, international normalized ratio; mRS, modified Rankin Scale; NIHSS, National Institute of Health Stroke Scale; TIA, transient ischemic attack; and WBC, white blood cell.

\*The values are statistically significant.

discerned an elevated CBV as a visually recognizable imaging marker or infarct patterns on the basis of reduced CBV area to facilitate a more straightforward and real-time approach.

The association between an increase in CBV and underlying ICAD can be attributed to an increase in vasodilation and the formation of vascular reservoirs as arterial stenosis progresses.<sup>13,14</sup> In the cascade of ischemic injury to the brain leading to cerebral infarction, initial vascular insult first reduces the perfusion pressure, followed by arteriolar dilation and capillary recruitment.<sup>15,16</sup> The concept of reactive vascular dilation in hypoperfused regions implies that perfusion maps can exhibit an elevation in CBV. This physiological response is not restricted to ICAD LVOS alone, as it signifies the initial phase of compensating for hemodynamic stress by increasing CBV.<sup>17</sup>

An increase in CBV in patients with ICAD may also reflect the development of collateralization. Unlike sudden embolic occlusion, intracranial stenosis progression that occurs over time allows collaterals to develop to sustain downstream perfusion from the culprit site, resulting in a lesser infarct core on ICAD LVOS. The measurement of the degree of collateral in clinical practice has primarily focused on arterial angiographical findings. Using CT angiography, the degree of collaterals can be graded according to the delay in the peripheral vessel filling in multiphase CT and distal reconstitution sites.<sup>18–20</sup> To overcome the limitations of these collateral grading systems that reflect only the arterial inflow, venous components of the collaterals were also considered in some studies,<sup>21</sup> and they were supported by the rationale that the consideration of combined arterial and venous collaterals may reflect the actual perfusion through the microcirculation.<sup>22</sup> In symptomatic ICAD, the effort to measure and grade the degree of collateral circulation has successfully demonstrated an association with the cerebral perfusion status,<sup>23</sup> suggesting a pivotal role of collateral circulation in the pathophysiology of ICAD.

In addition to the potential association of an increase in CBV with upregulation of vascular reservoir and collateral circulation, a severely decreased CBV may also reflect the infarct core, representing

**Table 4. Logistic Regression Analysis for ICAD LVOS and CBV Parameters**

	Model 1		Model 2		Model 3	
	OR (95% CI)	P value	OR (95% CI)	P value	OR (95% CI)	P value
Age (per 1 y increase)	1.02 (0.99–1.05)	0.2260	1.01 (0.99–1.04)	0.3033	1.01 (0.99–1.04)	0.3525
Absence of atrial fibrillation (vs presence of atrial fibrillation)	3.76 (1.71–8.29)	0.0010	3.74 (1.70–8.24)	0.0010	3.61 (1.63–8.00)	0.0015
NIHSS (per score 1 increase)	0.93 (0.86–1.01)	0.0681	0.93 (0.86–1.00)	0.0614	0.94 (0.87–1.02)	0.1367
Hemoglobin (per 1 mg/dL increase)	1.00 (0.96–1.03)	0.8225	1.00 (0.96–1.03)	0.7997	1.00 (0.96–1.03)	0.8672
Truncal-type occlusion (vs branching-site occlusion)	5.93 (2.65–13.26)	<0.001	5.76 (2.57–12.89)	<0.001	5.38 (2.39–12.12)	<0.001
Increase in CBV (vs nonincrease)	2.87 (1.27–6.45)	0.0109				
Normal CBV infarct pattern (vs other infarct patterns)			2.85 (1.20–6.75)	0.0175		
An increase in CBV or normal CBV infarct pattern					3.13 (1.43–6.84)	0.0043
AUROC	0.83 (0.78–0.88)		0.83 (0.77–0.88)		0.83 (0.76–0.89)	

AUROC indicates area under the receiver operating characteristic curve; CBV, cerebral blood volume; ICAD, intracranial atherosclerotic disease; LVOS, large-vessel occlusion stroke; NIHSS, National Institute of Health Stroke Scale; and OR, odds ratio.

the nonviable tissue fate of ischemic stroke.<sup>24</sup> Several infarct patterns on diffusion-weighted imaging have been known to be related to ICAD strokes: artery-to-artery embolism (common), branch atheromatous disease (common), thrombotic occlusion (rare), and hemodynamic impairment (rare).<sup>25</sup> Regarding ICAD LVOS, border zone and scattered infarct patterns were reportedly more frequently, whereas territorial infarct pattern was more frequent in embolic LVOS on diffusion-weighted imaging.<sup>26</sup> In the current study, we aimed to identify a representative infarct pattern on CBV map because perfusion imaging has been widely used for patient selection in EVT. We found that infarct patterns on CBV could not be clearly delineated as on diffusion-weighted imaging. A scattered infarct pattern was not visible, and a typical border zone infarct pattern was not clearly visible on the CBV-based infarct patterns. As for the normal CBV infarct pattern, the nonreduction in CBV within the penumbra, as measured by quantitative methods, or the second-pass effect of contrast agents in occluded vessels may often underestimate the actual infarct core.<sup>27–29</sup> Nevertheless, normal CBV infarct pattern accounted for a high proportion of ICAD as an underlying cause and was demonstrated as an independent predictor of ICAD LVOS. In addition, a normal CBV infarct pattern was associated with scattered, basal ganglia-only, and border zone infarct patterns on diffusion-weighted imaging.

An increase in the CBV may be associated with good clinical outcomes. To adjust for confounders in logistic regression analyses, covariables were mostly baseline factors, and ICAD as an underlying cause was incorporated; however, major determinants of clinical outcomes after EVT, such as reperfusion degree and symptomatic intracranial hemorrhage, were not incorporated in

the current study. Nevertheless, the increase in CBV states in the hypoperfused area was independently associated with good clinical outcomes, independent of the ICAD as an underlying cause. Increased vascular reservoirs and collaterals may lead to better clinical outcomes with LVOS and EVT.<sup>30</sup> This result may be indirectly attributed to the ICAD as an underlying cause of the occlusion; however, it was reported that patients with ICAD have a relatively poorer prognosis in LVOS,<sup>11</sup> and our study showed similar results. Despite a more favorable baseline neurological status in ICAD, those who receive EVT may experience longer procedure times, complex procedures, and mandatory antiplatelet treatment even after thrombolysis, which may result in relatively poorer outcomes.<sup>11,31,32</sup>

Our study has a few limitations. First, nordicICE software (NordicNeuroLab) for the current study did not support  $T_{max}$  maps. The use of  $T_{max}$  maps as a marker of critical hypoperfusion has been reported in the literature; however, we were unable to conduct a comparison between CBV and  $T_{max}$  maps. Future studies using software programs with delay-independent MTT maps and access to  $T_{max}$  parameters could further explore the utility of different perfusion parameters in predicting ICAD. Second, we used a qualitative CBV assessment with a modest interrater agreement. While previous studies have used quantitative parameters, such as  $T_{max}$ , we employed a qualitative approach for simplicity and ease of use in a clinical setting. This qualitative assessment can be subjective and prone to interrater variability. Future studies should perform quantitative analysis to validate our findings. Finally, we did not conduct a formal assessment of collateral degree using digital subtraction angiography or a CT angiography-based collateral scoring system. In our EVT approaches, contrast injection by a strong pushing



force can migrate and wedge the clot distally, where mechanical thrombectomy may be more difficult. Instead, road map imaging using a weak pushing force is mostly used for EVT, although it cannot evaluate collateral circulations. Although we presumed that the CBV state reflects the collateral status, a more comprehensive evaluation of collateral circulation could provide additional insights.

In conclusion, the current study highlights the use of CBV maps as a useful point-of-care neuroimaging tool for predicting ICAD as an underlying cause of LVOS. The increase in CBV or a normal CBV infarct pattern may indicate the presence of vasodilation-mediated blood reservoirs and increased collateral, as well as a smaller infarct core in ICAD LVOS. Moreover, an increase in CBV can also be used as a helpful marker not only for predicting ICAD as the underlying cause but also for clinical outcomes.

## ARTICLE INFORMATION

Received August 31, 2023; accepted October 23, 2023.

### Affiliations

Department of Brain Science, Ajou University School of Medicine, Suwon, Republic of Korea (S.K., H.K.K., J.Y.C.); Department of Neurology, Ajou University School of Medicine, Ajou University Hospital, Suwon, Republic of Korea (S.K., S.Y.P., J.Y.C., M.K., S.-J.L., J.M.H., J.S.L.); Department of Neurology, UCLA Comprehensive Stroke Center, Los Angeles, CA (D.S.L.); and Department of Radiology, Ajou University School of Medicine, Ajou University Hospital, Suwon, Republic of Korea (J.W.C.).

### Sources of Funding

None.

### Disclosures

None.

### Supplemental Material

Table S1.

Table S2.

## REFERENCES

1. Powers WJ, Rabinstein AA, Ackerson T, Adeoye OM, Bambakidis NC, Becker K, Biller J, Brown M, Demaerschalk BM, Hoh B, et al. 2018 guidelines for the early management of patients with acute ischemic stroke: a guideline for healthcare professionals from the American Heart Association/American Stroke Association. *Stroke*. 2018;49:e46–e110. doi: [10.1161/STR.000000000000158](https://doi.org/10.1161/STR.000000000000158)
2. Ko SB, Park HK, Kim BM, Heo JH, Rha JH, Kwon SU, Kim JS, Lee BC, Suh SH, Jung C, et al. 2019 update of the Korean clinical practice guidelines of stroke for endovascular recanalization therapy in patients with acute ischemic stroke. *J Stroke*. 2019;21:231–240. doi: [10.5853/jos.2019.00024](https://doi.org/10.5853/jos.2019.00024)
3. Lee JS, Hong JM, Kim JS. Diagnostic and therapeutic strategies for acute intracranial atherosclerosis-related occlusions. *J Stroke*. 2017;19:143–151. doi: [10.5853/jos.2017.00626](https://doi.org/10.5853/jos.2017.00626)
4. Lee JS, Lee S-J, Hong JM, Alverne FJAM, Lima FO, Nogueira RG. Endovascular treatment of large vessel occlusion strokes due to intracranial atherosclerotic disease. *J Stroke*. 2022;24:3–20. doi: [10.5853/jos.2021.01375](https://doi.org/10.5853/jos.2021.01375)
5. Baek JH, Kim BM. Angiographical identification of intracranial, atherosclerosis-related, large vessel occlusion in endovascular treatment. *Front Neurol*. 2019;10:298. doi: [10.3389/fneur.2019.00298](https://doi.org/10.3389/fneur.2019.00298)
6. Arenillas JF, Cortijo E, Garcia-Bermejo P, Levy EI, Jahan R, Liebeskind D, Goyal M, Saver JL, Albers GW. Relative cerebral blood volume is associated with collateral status and infarct growth in stroke patients in SWIFT PRIME. *J Cereb Blood Flow Metab*. 2018;38:1839–1847. doi: [10.1177/0271678X17740293](https://doi.org/10.1177/0271678X17740293)
7. Wintermark M, Flanders AE, Velthuis B, Meuli R, van Leeuwen M, Goldsher D, Pineda C, Serena J, van der Schaaf I, Waaijjer A, et al. Perfusion-CT assessment of infarct core and penumbra: receiver operating characteristic curve analysis in 130 patients suspected of acute hemispheric stroke. *Stroke*. 2006;37:979–985. doi: [10.1161/01.STR.0000209238.61459.39](https://doi.org/10.1161/01.STR.0000209238.61459.39)
8. Baek JH, Kim BM, Kim DJ, Heo JH, Nam HS, Song D, Bang OY. Importance of truncal-type occlusion in stentriever-based thrombectomy for acute stroke. *Neurology*. 2016;87:1542–1550. doi: [10.1212/WNL.0000000000003202](https://doi.org/10.1212/WNL.0000000000003202)
9. Lee SJ, Hong JM, Choi JW, Kang DH, Kim YW, Kim YS, Hong JH, Yoo J, Kim CH, Sohn SI, et al. CTA-based truncal-type occlusion is best matched with postprocedural fixed focal stenosis in vertebralbasilar occlusions. *Front Neurol*. 2018;9:1195. doi: [10.3389/fneur.2018.01195](https://doi.org/10.3389/fneur.2018.01195)
10. Kim M, Lee S-J, Park SY, Hong JM, Lee JS. A novel etiological classification in patients with intracranial large vessel occlusion and endovascular treatment: discordance with the classic and SSS TOAST systems: a retrospective cohort study. *Precis Future Med*. 2023;7:83–89. doi: [10.23838/pfm.2023.00065](https://doi.org/10.23838/pfm.2023.00065)
11. Lee JS, Lee SJ, Yoo JS, Hong JH, Kim CH, Kim YW, Kang DH, Kim YS, Hong JM, Choi JW, et al. Prognosis of acute intracranial atherosclerosis-related occlusion after endovascular treatment. *J Stroke*. 2018;20:394–403. doi: [10.5853/jos.2018.01627](https://doi.org/10.5853/jos.2018.01627)
12. Haussen DC, Bousslama M, Dehkharghani S, Grossberg JA, Bianchi N, Bowen M, Frankel MR, Nogueira RG. Automated CT perfusion prediction of large vessel acute stroke from intracranial atherosclerotic disease. *Interv Neurol*. 2018;7:334–340. doi: [10.1159/000487335](https://doi.org/10.1159/000487335)
13. Levin DC, Beckmann CF, Serur JR. Vascular resistance changes distal to progressive arterial stenosis: a critical re-evaluation of the concept of vasodilator reserve. *Invest Radiol*. 1980;15:120–128. doi: [10.1097/00004424-198003000-00005](https://doi.org/10.1097/00004424-198003000-00005)
14. Beckmann CF, Levin DC, Kubicka R. Reactive hyperemia as an indicator of peripheral vasodilation associated with arterial stenoses. *Invest Radiol*. 1982;17:77–81. doi: [10.1097/00004424-198201000-00015](https://doi.org/10.1097/00004424-198201000-00015)
15. Astrup J, Siesjo BK, Symon L. Thresholds in cerebral ischemia—the ischemic penumbra. *Stroke*. 1981;12:723–725. doi: [10.1161/01.STR.12.6.723](https://doi.org/10.1161/01.STR.12.6.723)
16. Heiss WD. Ischemic penumbra: evidence from functional imaging in man. *J Cereb Blood Flow Metab*. 2000;20:1276–1293. doi: [10.1097/0004647-200009000-00002](https://doi.org/10.1097/0004647-200009000-00002)
17. Muir KW, Baird-Gunning J, Walker L, Baird T, McCormick M, Coutts SB. Can the ischemic penumbra be identified on noncontrast CT of acute stroke? *Stroke*. 2007;38:2485–2490. doi: [10.1161/STROKEAHA.107.484592](https://doi.org/10.1161/STROKEAHA.107.484592)
18. Garcia-Tornel A, Carvalho V, Boned S, Flores A, Rodriguez-Luna D, Pagola J, Muchada M, Sanjuan E, Coscojuela P, Juega J, et al. Improving the evaluation of collateral circulation by multiphase computed tomography angiography in acute stroke patients treated with endovascular reperfusion therapies. *Interv Neurol*. 2016;5:209–217. doi: [10.1159/000448525](https://doi.org/10.1159/000448525)
19. Christoforidis GA, Mohammad Y, Kehagias D, Avutu B, Slivka AP. Angiographic assessment of pial collaterals as a prognostic indicator following intra-arterial thrombolysis for acute ischemic stroke. *AJNR Am J Neuroradiol*. 2005;26:1789–1797.
20. Higashida RT, Furlan AJ, Roberts H, Tomsick T, Connors B, Barr J, Dillon W, Warach S, Broderick J, Tilley B, et al. Trial design and reporting standards for intra-arterial cerebral thrombolysis for acute ischemic stroke. *Stroke*. 2003;34:e109–e137. doi: [10.1161/01.STR.0000082721.62796.09](https://doi.org/10.1161/01.STR.0000082721.62796.09)
21. Parthasarathy R, Sohn SI, Jeerakathil T, Kate MP, Mishra SM, Nambiar VK, Ahmad A, Menon BK, Shuaib A. A combined arterial and venous grading scale to predict outcome in anterior circulation ischemic stroke. *J Neuroimaging*. 2015;25:969–977. doi: [10.1111/jon.12260](https://doi.org/10.1111/jon.12260)
22. Munuera J, Blasco G, Hernandez-Perez M, Daunis IEP, Davalos A, Liebeskind DS, Wintermark M, Demchuk A, Menon BK, Thomalla G, et al. Venous imaging-based biomarkers in acute ischaemic stroke. *J Neurol Neurosurg Psychiatry*. 2017;88:62–69. doi: [10.1136/jnnp-2016-314814](https://doi.org/10.1136/jnnp-2016-314814)
23. Liebeskind DS, Cotsonis GA, Saver JL, Lynn MJ, Cloft HJ, Chimowitz MI. Warfarin-aspirin symptomatic intracranial disease I. Collateral

- circulation in symptomatic intracranial atherosclerosis. *J Cereb Blood Flow Metab.* 2011;31:1293–1301. doi: [10.1038/jcbfm.2010.224](https://doi.org/10.1038/jcbfm.2010.224)
24. Hossmann KA. Viability thresholds and the penumbra of focal ischemia. *Annals Neurol.* 1994;36:557–565. doi: [10.1002/ana.410360404](https://doi.org/10.1002/ana.410360404)
  25. Bang OY. Intracranial atherosclerosis: current understanding and perspectives. *J Stroke.* 2014;16:27–35. doi: [10.5853/jos.2014.16.1.27](https://doi.org/10.5853/jos.2014.16.1.27)
  26. Suh HI, Hong JM, Lee KS, Han M, Choi JW, Kim JS, Demchuk AM, Lee JS. Imaging predictors for atherosclerosis-related intracranial large artery occlusions in acute anterior circulation stroke. *J Stroke.* 2016;18:352–354. doi: [10.5853/jos.2016.00283](https://doi.org/10.5853/jos.2016.00283)
  27. Wintermark M, Reichhart M, Thiran JP, Maeder P, Chalaron M, Schnyder P, Bogousslavsky J, Meuli R. Prognostic accuracy of cerebral blood flow measurement by perfusion computed tomography, at the time of emergency room admission, in acute stroke patients. *Ann Neurol.* 2002;51:417–432. doi: [10.1002/ana.10136](https://doi.org/10.1002/ana.10136)
  28. Wintermark M, Reichhart M, Cuisenaire O, Maeder P, Thiran JP, Schnyder P, Bogousslavsky J, Meuli R. Comparison of admission perfusion computed tomography and qualitative diffusion- and perfusion-weighted magnetic resonance imaging in acute stroke patients. *Stroke.* 2002;33:2025–2031. doi: [10.1161/01.str.0000023579.61630.ac](https://doi.org/10.1161/01.str.0000023579.61630.ac)
  29. Copen WA, Schaefer PW, Wu O. MR perfusion imaging in acute ischemic stroke. *Neuroimaging Clin N Am.* 2011;21(259–283):x–83, x. doi: [10.1016/j.nic.2011.02.007](https://doi.org/10.1016/j.nic.2011.02.007)
  30. Lee JS, Bang OY. Collateral status and outcomes after thrombectomy. *Transl Stroke Res.* 2022;14:22–37. doi: [10.1007/s12975-022-01046-z](https://doi.org/10.1007/s12975-022-01046-z)
  31. Lee JS, Hong JM, Lee KS, Suh HI, Choi JW, Kim SY. Primary stent retrieval for acute intracranial large artery occlusion due to atherosclerotic disease. *J Stroke.* 2016;18:96–101. doi: [10.5853/jos.2015.01347](https://doi.org/10.5853/jos.2015.01347)
  32. Baek JH, Kim BM, Heo JH, Kim DJ, Nam HS, Kim YD. Outcomes of endovascular treatment for acute intracranial atherosclerosis-related large vessel occlusion. *Stroke.* 2018;49:2699–2705. doi: [10.1161/STROKEAHA.118.022327](https://doi.org/10.1161/STROKEAHA.118.022327)